

PUC

Series: Monographs in Computer Science
and Computer Applications

Nº 2/69

AN ITERATIVE COMPUTER SOLUTION FOR THE EQUATIONS OF ELASTIC WALL-GIRDERS

by

JAMME MASON - JOSÉ ROBERTO RIBEIRO DOS SANTOS

Computer Science Department - Rio Datacenter

CENTRO TECNICO CIENTIFICO
Pontificia Universidade Católica do Rio de Janeiro
Rua Marques de São Vicente, 209 — ZC 20
Rio de Janeiro — Brasil

Simão Simões Jorani - 1969

AN ITERATIVE COMPUTER SOLUTION FOR THE EQUATIONS OF ELASTIC WALL-GIRDERS (1)

JAYME MASON - JOSÉ ROBERTO RIBEIRO DOS SANTOS
COMPUTER SCIENCE DEPARIMENT
PUC - RIO DE JANEIRO

AN ITERATIVE COMPUTER SOLUTION FOR THE EQUATIONS OF ELASTIC WALL-GIRDERS (1)

JAYME MASON (2)

JOSÉ ROBERTO RIBEIRO DOS SANTOS (2)

ABSTRACT

This report presents a computer solution of the elliptic differential equations of elastic wall-girder theory.

The method of solution is iterative and overrelaxation is used in order to speed up convergence.

Two kinds of boundary conditions are accounted for. The results of the calculations will be commented and comparisons will be made with related known solutions.

1. Introduction

The well known theory of two dimensional elasticity [1] gives the biharmonic equation

$$\frac{\partial^4 F(x,y)}{\partial x^4} + 2 \frac{\partial^4 F(x,y)}{\partial x^2 \partial y^2} + \frac{\partial^4 F(x,y)}{\partial x^2} = 0 \quad (1)$$

as a basis for the determination of the stress pattern in a wall-girder. In the above equation, $F(x,y)$ is a stress function, from which it is possible to derive the components of stress:

$$\tau_{xy} = - \frac{\partial F(x,y)}{\partial x \partial y}, \quad \sigma_x = \frac{\partial^2 F(x,y)}{\partial y^2}, \quad \sigma_y = \frac{\partial^2 F(x,y)}{\partial x^2} \quad (2)$$

(1) The idea of the present investigation was derived from a design by the architect Sérgio Bernardes, namely a building for the Telephone Company of Belém, Brazil.

(2) Professor of Engineering Mechanics PUC-Rio de Janeiro, Associate - Professor of Applied - Mathematics Computer Science Department - PUC-Rio de Janeiro.

If the material distribution in the girder is not continuous, the central term of equation(1) must be slightly modified.

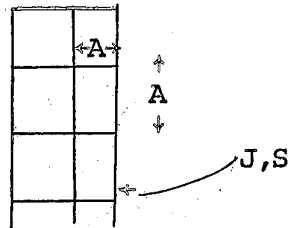


Fig. 1

Suppose the wall girder is made up of a grid of bars as suggested in Fig. 1 the mesh width being equal to A . It is assumed that the strength properties of the bars is given by J and S , respectively the moment of inertia and the cross sectional area of the bars.

Under these assumptions, the equation (1) must be changed to 2

$$\frac{\partial^4 F(x,y)}{\partial x^4} + c \frac{\partial^4 F(x,y)}{\partial x^2 \partial y^2} + \frac{\partial^4 F(x,y)}{\partial y^4} = 0 \quad (3)$$

where

$$c = \frac{A^2 S}{6 J} \quad (4)$$

The latter alternative has found recently some architectural applications, as in the design leading to the idea of the present investigation.

2. Boundary Conditions

A wide variety of boundary conditions would be possible, but only two particular situations are examined, on account of their physical interest.

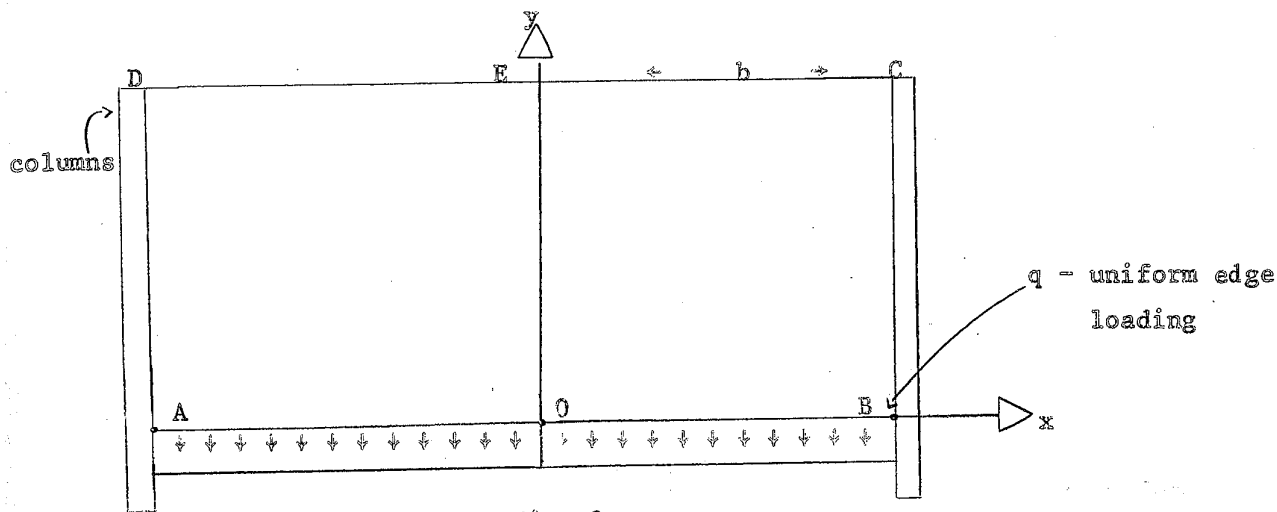


Fig. 2

The conditions of support for the wall-girder in the architectural design are sketched in Fig. 2. The girder is supported at the ends over the whole height, on two columns and a uniform load q may be assumed to be applied in the lower edge. The upper edge is free of loading.

In a first approximation, we assume that the column reactions are uniformly distributed over the depth of the girder, as in the figure below (Fig. 3)

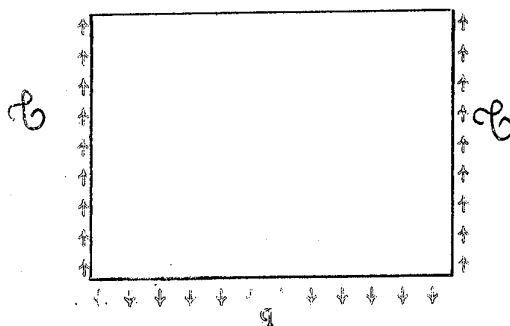


Fig. 3 (Case 1)

As such an assumption is to a certain extent arbitrary, it must be checked as soon as the calculations are completed.

A second and more realistic boundary condition along the column may be introduced. We may assume that the wall is stiffly connected to the columns and that the longitudinal strain in the column is negligible. In such a case, the vertical strains in the adjoining vertical section of the wall may be set equal to zero. Then the vertical stress σ_y , will also be approximately zero as a consequence of Hooke's law, so that:

$$\sigma_y = \frac{\partial^2 F(x,y)}{\partial x^2} = 0$$

along a vertical boundary (Case 2).

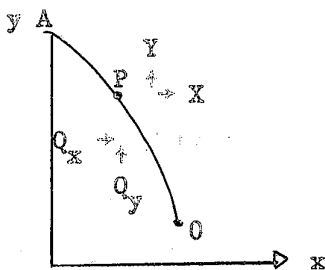


Fig. 4

We shall now discuss briefly the boundary conditions along the edges in which external loads are specified. In such a case we know that the boundary values of the stress function F and its derivatives at a point P , as in Fig. 4 are given by [3].

$$\frac{\partial F(x,y)}{\partial x} = -Q_y, \quad \frac{\partial F(x,y)}{\partial y} = Q_x$$

$$F(x,y) = M_p \tag{5}$$

Q_x is the resultant of the edge loading in the direction of the x -axis, computed between an assumed origin O and on arbitrary contour point P , ie,

$$Q_x = \int_0^P X ds$$

A similar definition is applicable for Q_y :

$$Q_y = \int_0^P Y ds$$

As for M , it is the moment of the contour forces between O and P , with respect to P , positive if counterclockwise.

It is considered that the girder is in equilibrium and point O of Fig. 1 is

taken as the origin, thus it is possible to obtain the boundary conditions for the two cases with the aid of formulas (5):

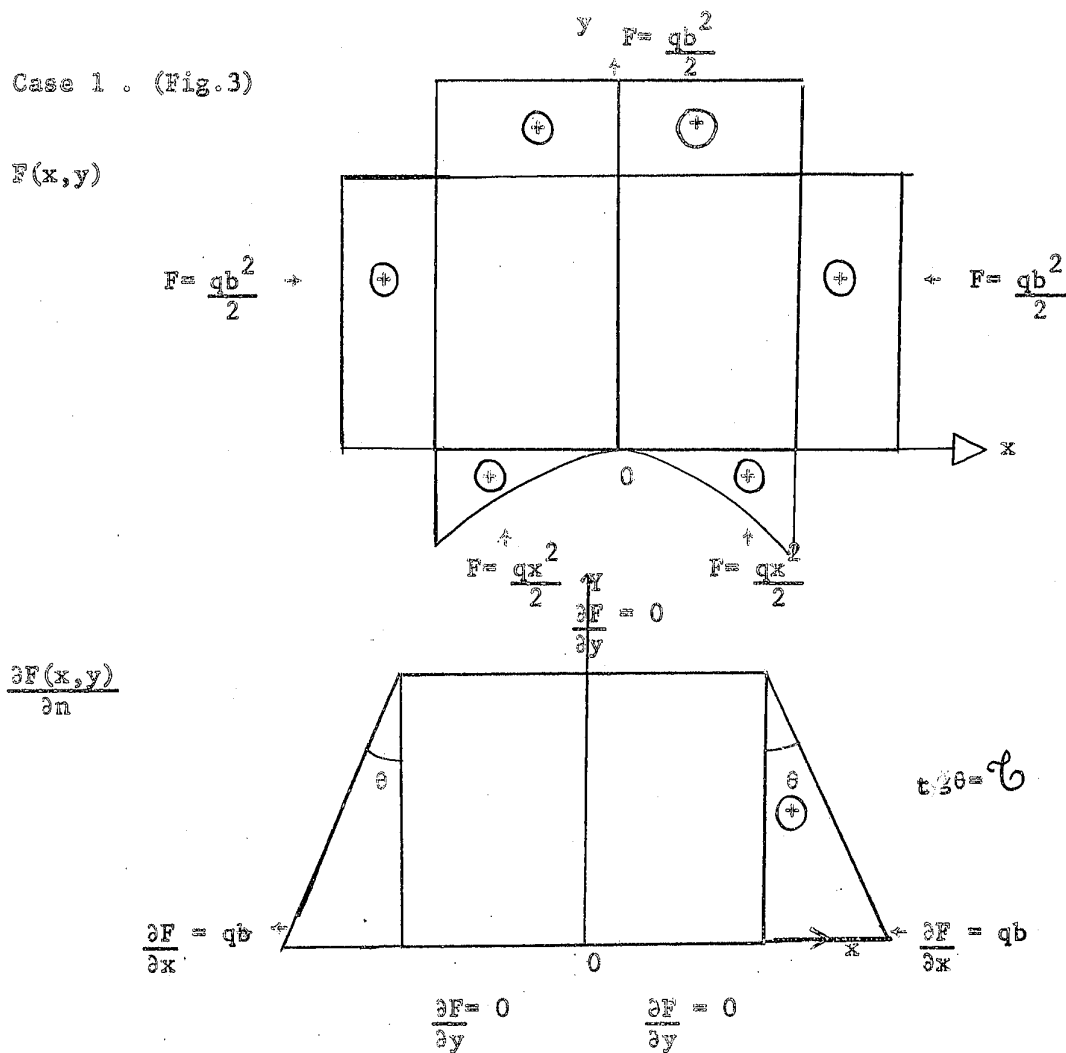
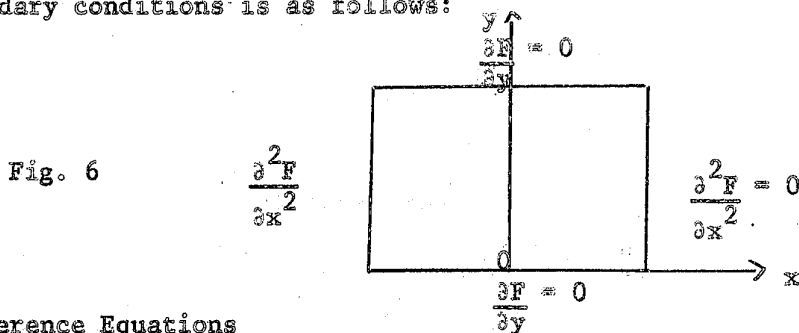


Fig. 5

Case 2 -

The boundary conditions for $F(x,y)$ for case 2 are the same as Case 1. The second boundary conditions is as follows:



3. Difference Equations

Taylor's series are used to have a second order difference equation for the differential equation (3). If a uniform square mesh of side D in the ABCD region of Fig. 2 is chosen, for a point 0, as in Fig. 7, we shall have

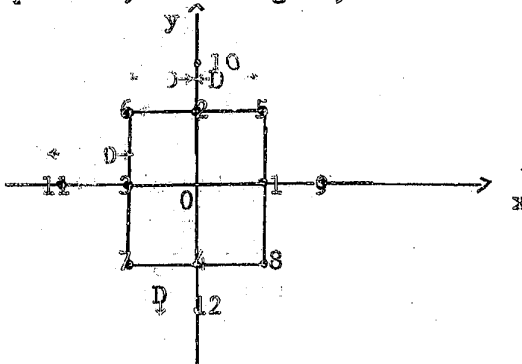


Fig. 7

$$(12 + 4c) F_0 = (4 + 2c) \sum_{i=1}^4 F_i - c \sum_{i=5}^8 F_i - \frac{1}{2} \sum_{i=9}^{12} F_i \quad (7)$$

If C equals 2, formula (7) reduces to the well known second order difference equation for the biharmonic equation:

$$20 F_0 = 8 \sum_{i=1}^4 F_i - 2 \sum_{i=5}^8 F_i - \sum_{i=9}^{12} F_i \quad (8)$$

Formulas (7) and (8), take on a slightly different form, for points near the boundary. By considering formula (7), it comes out as follows:

a) Point 0 of Fig. 7 near the AB edge (cases 1 and 2), Fig. 2.

$$(13+4c) F_0 = (4+2c) \sum_{i=1}^4 F_i - c \sum_{i=5}^8 F_i - \sum_{i=9}^{11} F_i$$

b) Point 0 near the CD edge (cases 1 and 2)

$$(13+4c) F_0 = (4+2c) \sum_{i=1}^4 F_i - c \sum_{i=5}^8 F_i - \sum_{\substack{i=9 \\ i \neq 10}}^{12} F_i$$

c) Point 0 near the BC edge (Case 1)

$$(13+4c) F_0 = (4+2c) \sum_{i=1}^4 F_i - c \sum_{i=5}^8 F_i - \sum_{i=10}^{12} F_i - 2D \frac{\partial F}{\partial y} \Big|_1$$

d) Point 0 near the BC edge (Case 2)

$$(11+4c) F_0 = (4+2c) \sum_{i=1}^4 F_i + c \sum_{i=5}^8 F_i + \sum_{i=10}^{12} F_i - 2 F_1$$

e) Point 0 near the corner B (Case 1)

$$(14+4c) F_0 = (4+2c) \sum_{i=1}^4 F_i - \sum_{i=5}^8 F_i - \sum_{i=10}^{11} F_i - 2 D \frac{\partial F}{\partial y} \Big|_1$$

f) Point 0 near the corner B (Case 2)

$$(12+4c) F_0 = (4+2c) \sum_{i=1}^4 F_i + c \sum_{i=5}^8 F_i + \sum_{i=10}^{11} F_i - 2 F_1$$

g) Point 0 near the corner C (Case 1)

$$(14+4c) F_0 = (4+2c) \sum_{i=1}^4 F_i - c \sum_{i=5}^8 F_i - \sum_{i=11}^{12} F_i - 2 D \frac{\partial F}{\partial y} \Big|_1$$

h) Point 0 near the corner C (Case 2)

$$(12+4c) F_0 = (4+2c) \sum_{i=1}^4 F_i + c \sum_{i=5}^8 F_i + \sum_{i=11}^{12} F_i - 2 F_1$$

4. COMPUTER PROGRAM

The boundary conditions for Cases 1 and 2 are symmetric with respect to the y-axis of Fig. 2. Thus, it is possible to limit the calculations for $F(x,y)$ only to the O B C E region.

It is known that, for the second order finite difference representation of the biharmonic equation, the point Gauss-Seidel method converges [4]. Even though it is not possible to find a mathematical expression for the optimum acceleration factor for the point relaxation, the Jacobi matrix is not consistently ordered p-cyclic [5]. For small mesh-side D , $W=1.8$ is a good approximation for the optimum acceleration factor W . The parameter C of equation (3), is, in the practical range always greater than 2. As a consequence, it is easy to see that the point Gauss-Seidel method converges.

The parameter $W=1.85$ was used in the computation and a great economy in time was achieved against the point Gauss-Seidel method, as it will be seen later. For example, for Case 2 with mesh of 10×20 the point over-relaxation took about 4 minutes against 13 minutes for the point Gauss-Seidel with a relative precision of 10^{-4} .

The number of iterations was such that

$$\left| \frac{F^{(n)}(I,J) - F^{(n-1)}(I,J)}{F^{(n)}(I,J)} \right| < \text{PREC}$$

for all (I,J) in the domain. The iterative process was started with $F^{(0)}(I,J) = 0$ for all (I,J) .

The program was written in FORTRAN IV for an IBM 7044 Computer.

5. Analysis of Results

As an illustration, the present computer program was used, in the calculation of the sample problems sketched in Fig. 8.

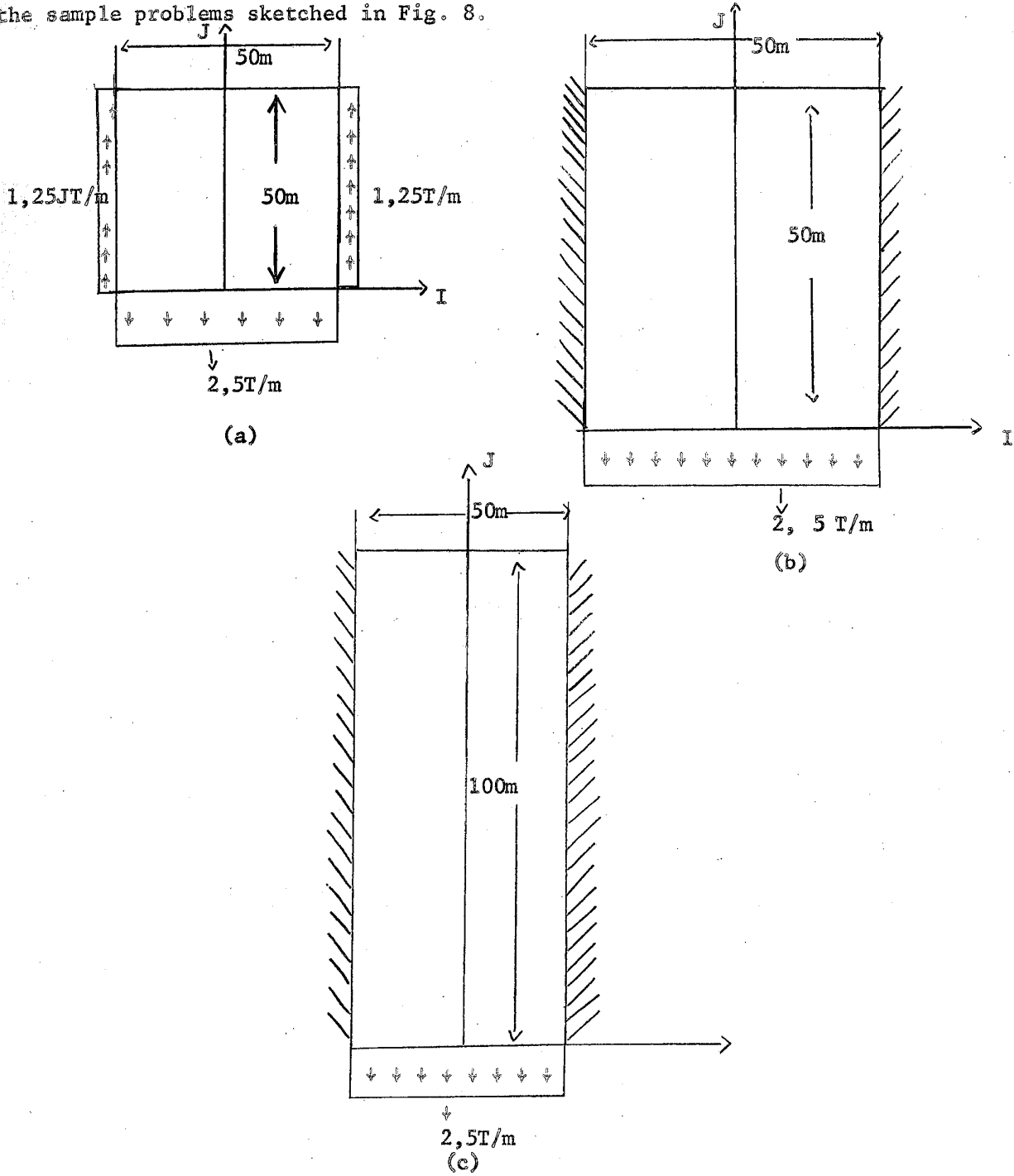


Fig. 8

Cases (a) and (b) are the same girder with different boundary conditions along the vertical edges. In case (a) the shearing stress is prescribed and in case (b) we assume fixity along the vertical boundaries.

Case (c) is the same as case (b) with the depth of the girder doubled. For all cases, the characteristics of the grid making up the wall-girder were given by the following values:

$$J = 0.010 \text{ m}^4, S = 0.10 \text{ m}^2, A = 2,5 \text{ m}$$

Cases (a) and (b) were solved for a mesh of 10×20 for half the domain. The main results are summarized in Fig. 9.

A analysis on the σ_x diagram in the Fig. 9 shows that the situation approaches very closely the case of a simply supported beam, according to the elementary theory. In fact, the stress diagrams are practically linear and a simple check with the help of the elementary formulas from the strength of materials would convince us that the results are correct.

Under the same conditions the σ_y stress decreases in the height as one should expect and these stresses carry the vertical load applied at the lower edge inside the wall girder.

Finally, the shearing stress diagram is very illuminating. At the center sections it comes very close to the parabolic distribution which is well known in the elementary beam theory. At the sections close to the support there is a very rapid transition from the assumed rectangular diagram to the parabolic distribution just mentioned. This should be in agreement with Saint-Venant principle in the Theory of Elasticity. According to such a principle, statically equivalent force distributions produce the same effect not far from the original application of the loads.

Therefore an assumed shearing stress distribution should have some implications only in the region close to the support, but it should not influence the results.

in the most important parts of the domain.

We can make sure of the above remarks if we compare the numerical results obtained for cases (a) and (b) in the region close to the center of the span of the wall-girder. However case (b) shows that the fixed boundary conditions alters substantially the stress distribution close to the vertical supports.

For purposes of comparison the results of case (c) are plotted in Fig. 10.

It should be evident to the expert that the stress diagrams approaches those of a typical wall girder of infinite height. One can remark that in the latter case, the program handled a system of 400 equations with 400 unknowns in about 15 minutes.

6. Conclusions

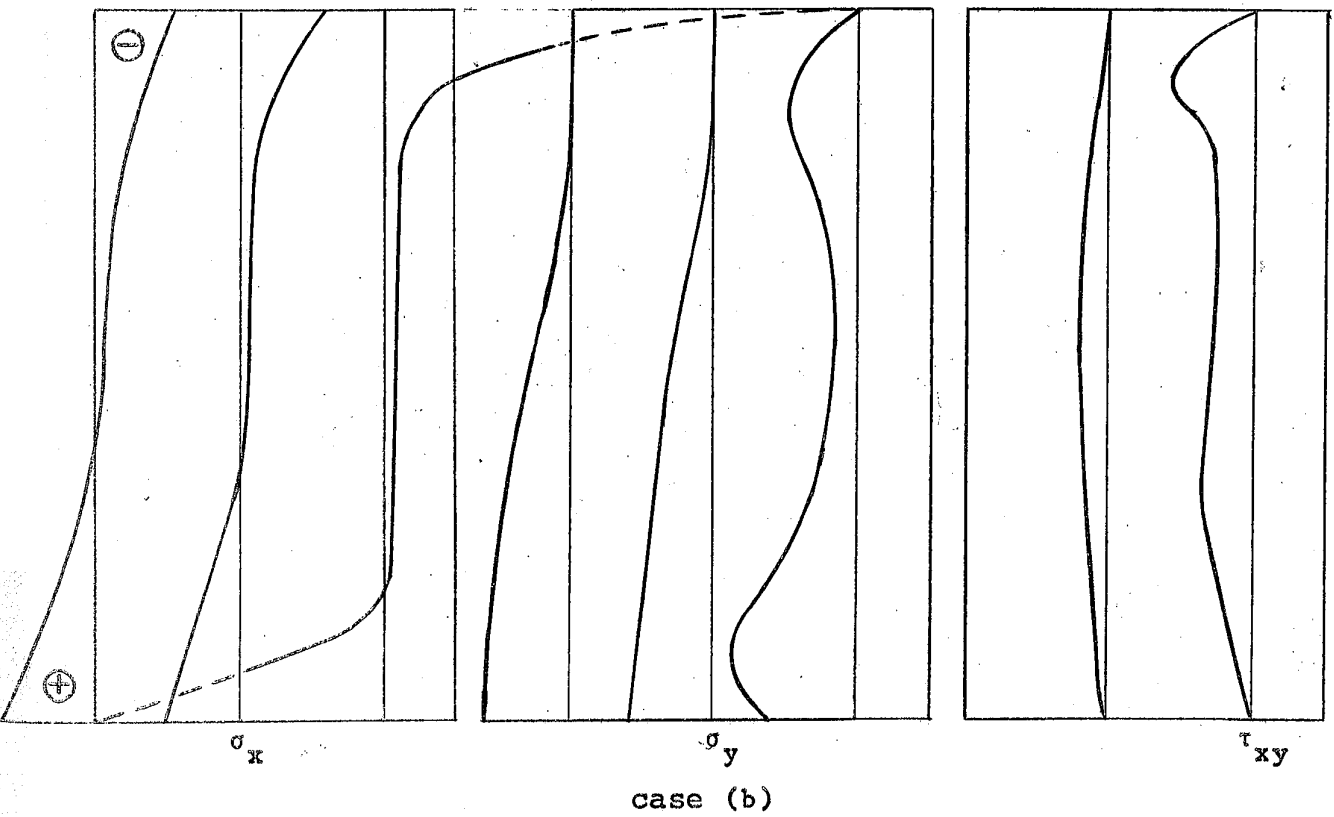
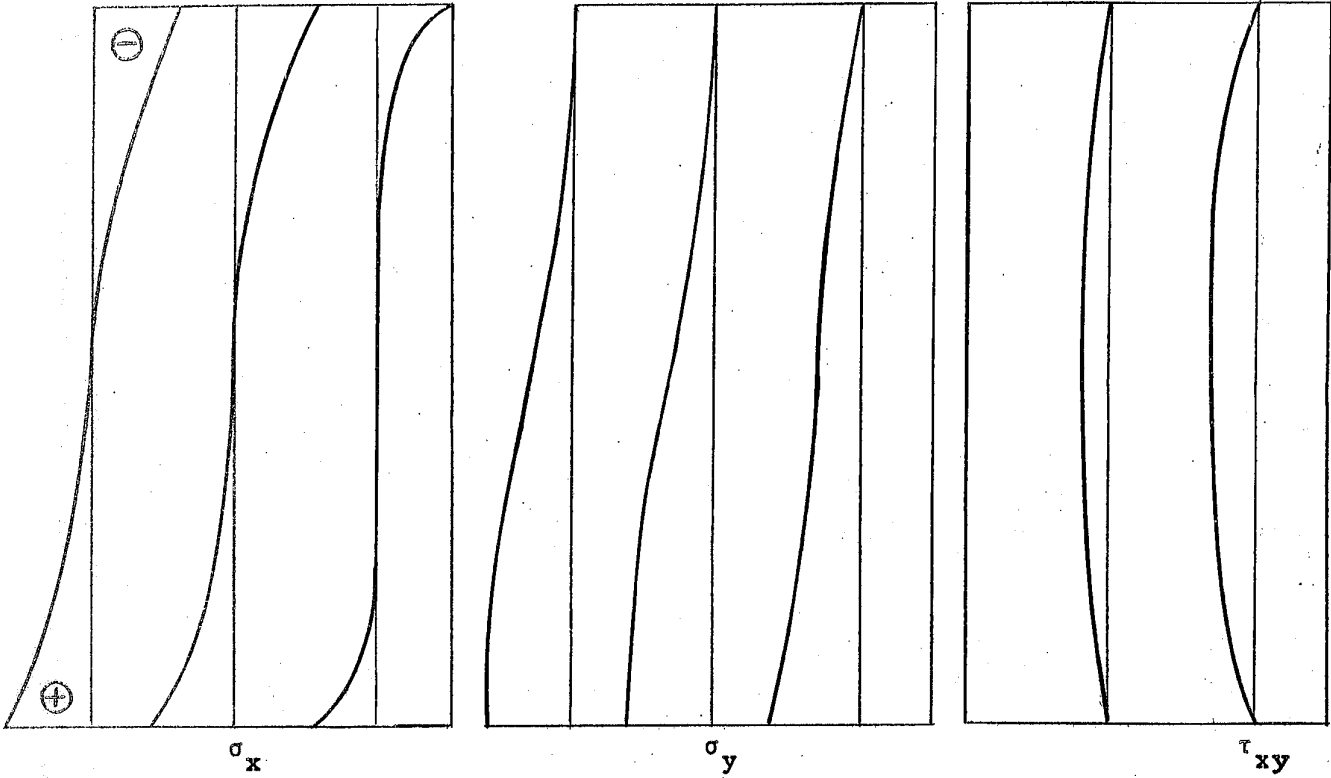
The results of the present investigation were compared with a calculation based upon the theory of framed structures, according to an IBM-1130 stress program. Both approaches were found to be in satisfactory agreement. As a conclusion it should be pointed out that iterative methods may be very convenient as soon as convergence can be ensured. Matrix problems of a very high dimension are dealt with property in this way.

REFERENCES

- [1]. Timoshenko - Goodier - "Theory of Elasticity"
Mc Graw Hill
- [2]. Mason, J. "Contribuição das Estruturas em Superfície Anisotropa", 1963
- [3]. Girkman, K. "Flachentragwerke" Springer Verlag - Wien
- [4]. Sadaca, K. "Solutions Numériques de L'Equation Biharmonique à deux variables"
Thesis - Univ. of Toulouse - 1967
- [5] Varga, R. "Matrix Iterative Analysis" - Prentice Hall - 1963.

(12a)

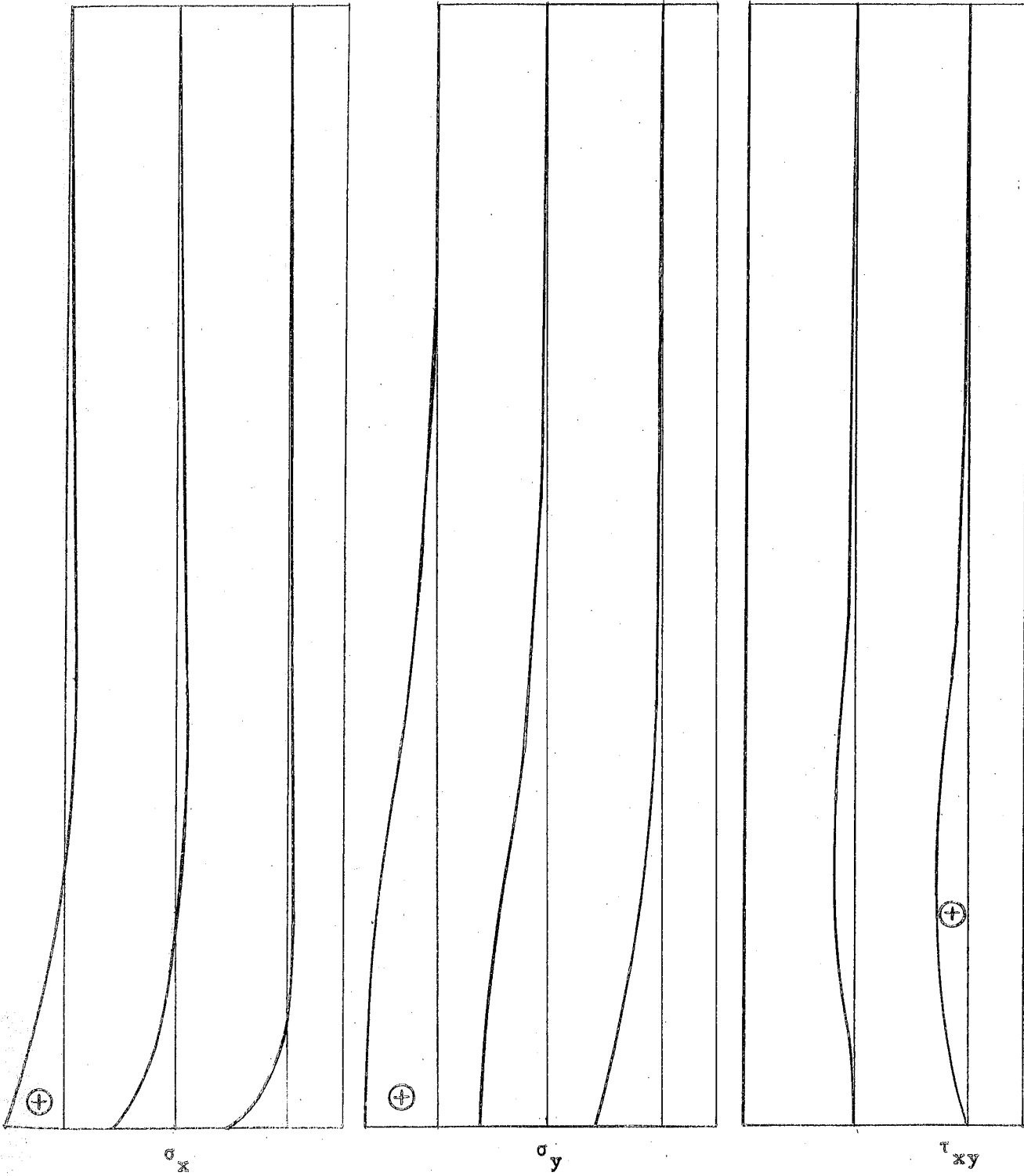
case (a)



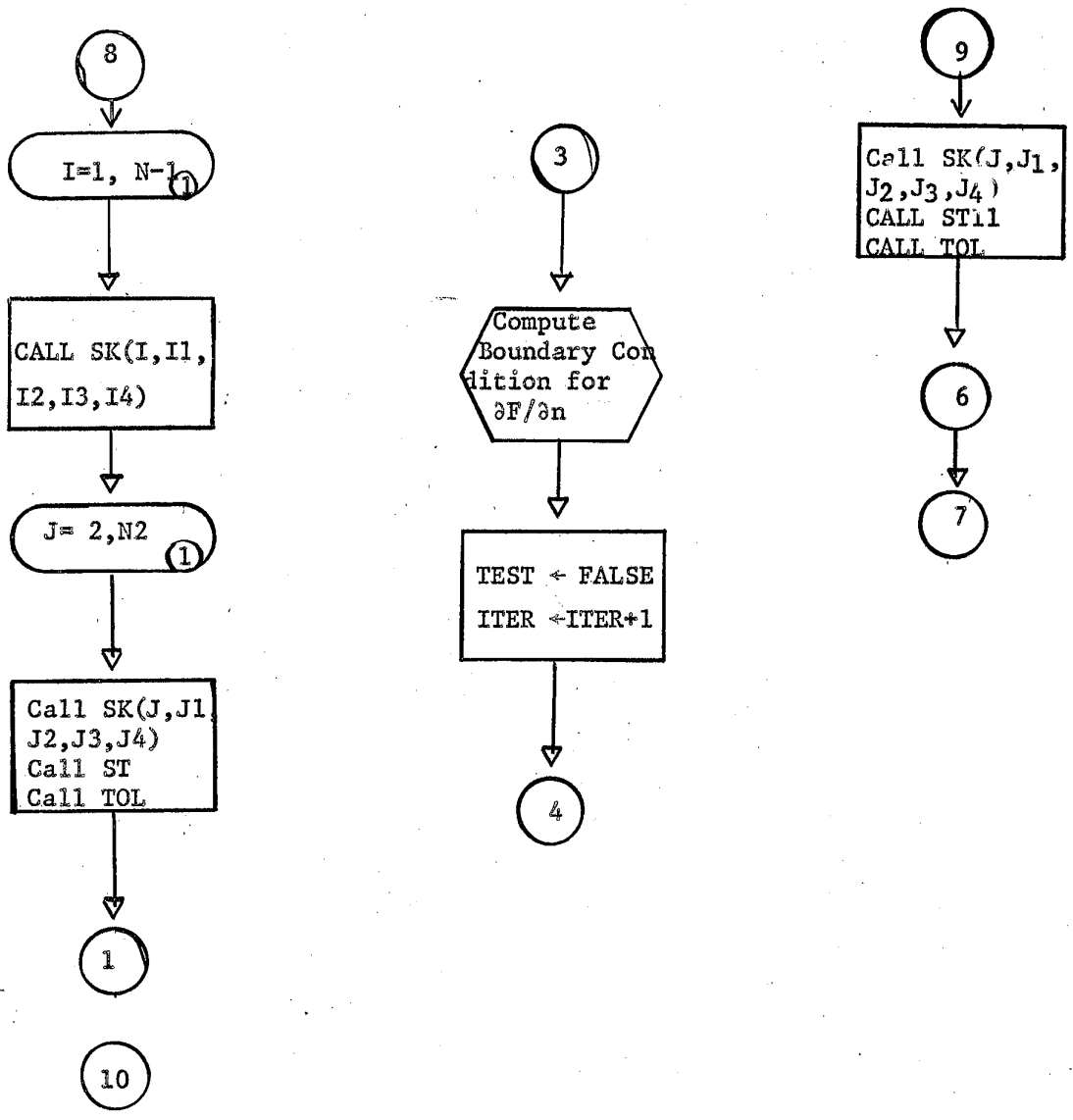
case (b)

(12b)

case (c)

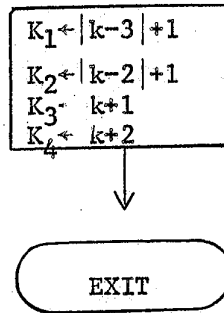


Flow Chart - Main Program (cont.)



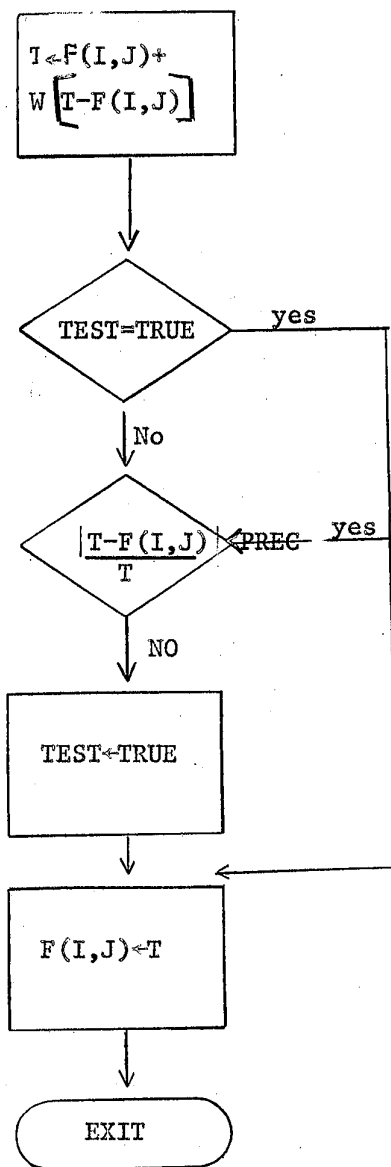
This subroutine computes the coordinates of points to be used in the difference equations it account for the problem symmetry.

Flow Chart - Procedure SK(k)



This subroutine computes a new value of F(I,J). An acceleration parameter is used. A test, in order to stop the iterative process, is also made.

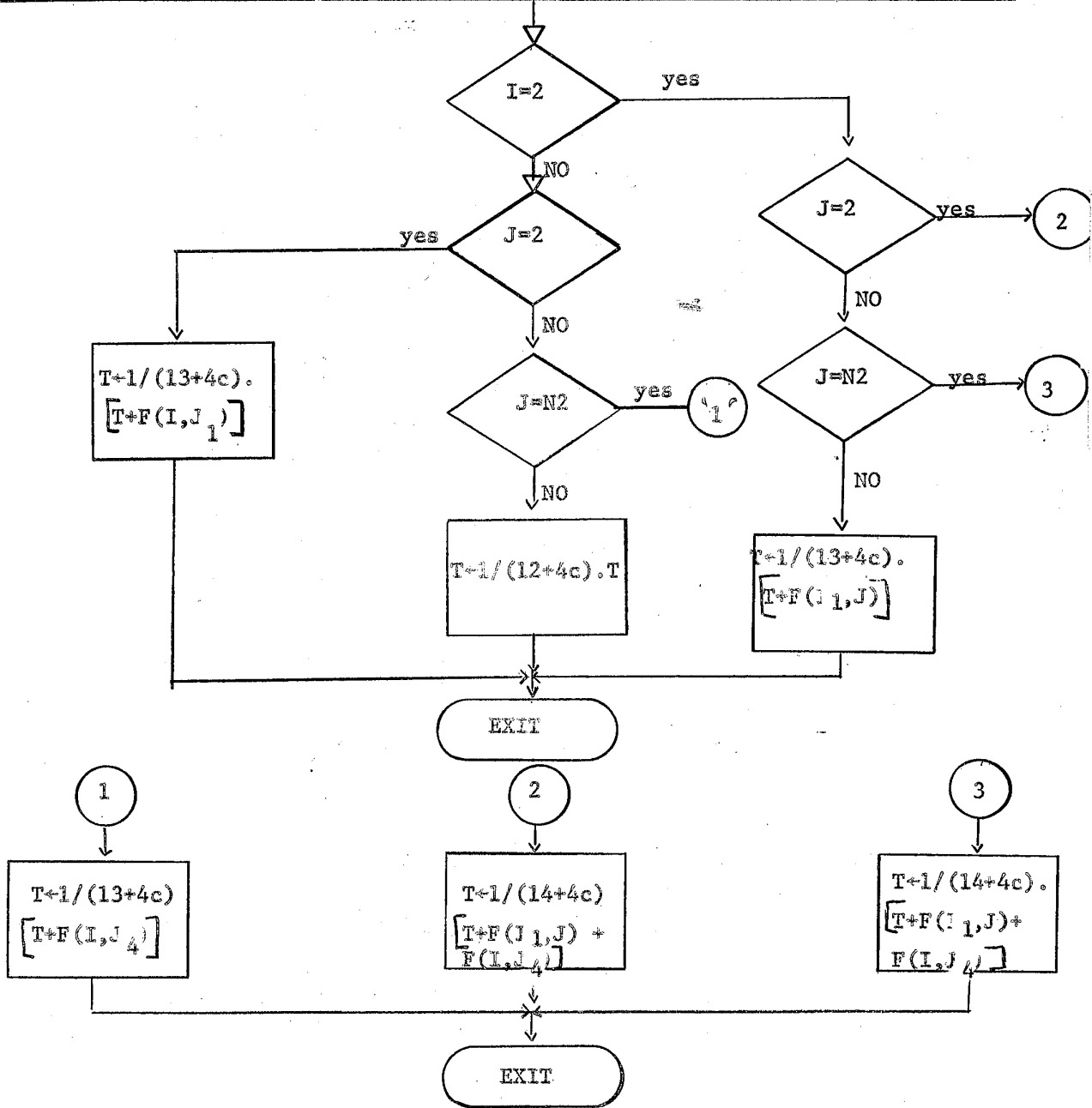
Procedure Tol



This subroutine computes an intermediate value for $F(I,J)$, to a point in the do main.

Procedure ST

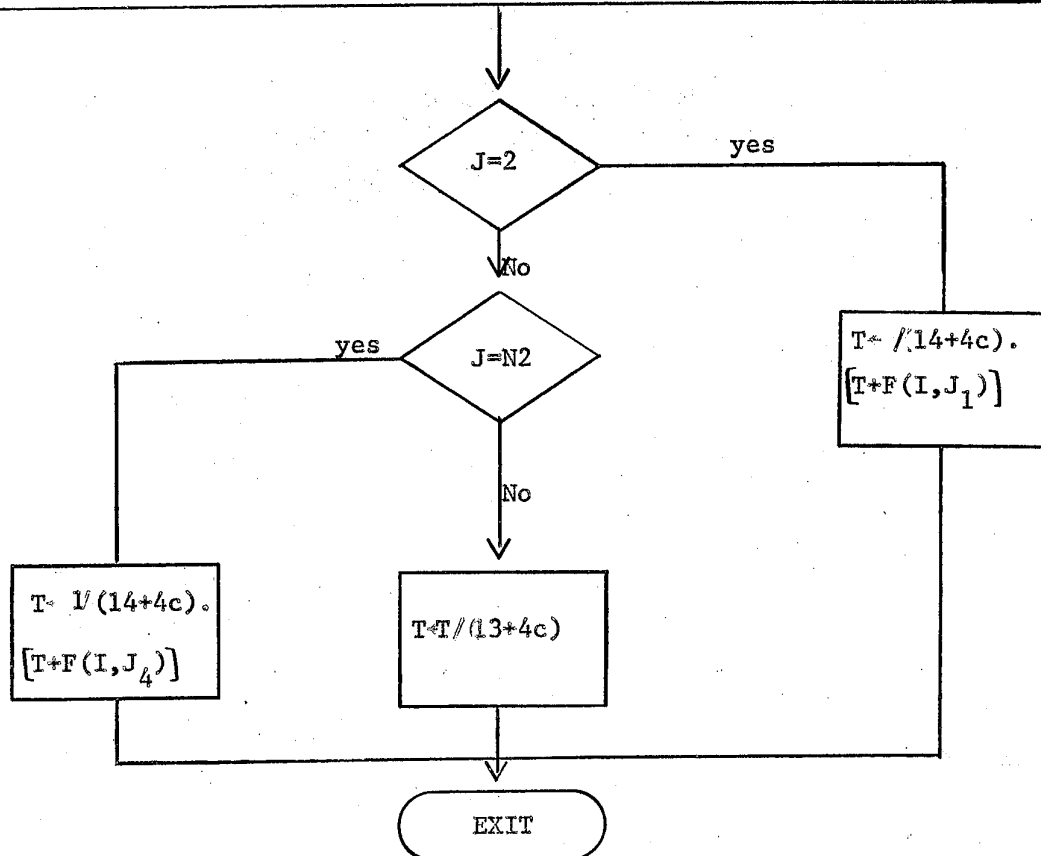
$$T \leftarrow (4-2c) \sum_{k=2}^3 F(I_k, J) + (F(I, J_k) - c_1 \sum_{k=2}^3 F(I_k, J_1) + \sum_{k=1}^4 [F(I_k, J) + F(I, J_k)]_{k \neq 2, 3})$$



This subroutine computes an intermediate value for $F(I,J)$, to a point near BC for case 1.

Procedure ST 11

$$T \leftarrow (4-2c) \sum_{k=2}^3 [F(J_k, J) + F(I, J_k)] - \left[c \sum_{1, k=2}^3 F(I_k, J_1) + \sum_{\substack{k=1 \\ k \neq 2, 3}}^4 [F(I, J_k) + F(I_1, J)] \right] - TAV(J)$$



This subroutine computes an intermediate value for $F(I,J)$, to a point near EC for case 2.

Flow-Chart - Procedure ST1

